Input Resistance Changes and Related Performances of a Normal-Mode Helical Antenna in a Human Body Application

N. Q. Dinh [1], D. T. Dung [2], Y. Yamada [3], and N. Michishita [4]

[1] Faculty of Radio-Electronics Engineering
Le Quy Don Technical University, Hanoi, Vietnam
dinhnq@mta.edu.vn

[2] Telecommunication University, Khanhhoa, Vietnam
dangtiendung@tcu.edu.vn

[3]Malaysia-Japan International Institute of Technology
Universiti Teknologi Malaysia, Kuala Lumpur, Malaysia
yoshihide@utm.my

[4] Department of Electrical and Electronic Engineering
National Defense Academy, Yokosuka, Japan
naobumi@nda.ac.jp

Abstract ─ Recently, ingestible capsule endoscopy has been developed to ease the dosimetry process in the stomach and tract. In this application, a helical antenna is used because its shape is suitable for a capsule. The electric performance of a coil antenna can be analyzed by the normal-mode helical antenna (NMHA) concept. Previously, the design equations for NMHA have already been developed in free space application. Application of NMHA in the human body is innovative. Antenna design equations and electrical performance should be clarified. Presently, only self-resonant structure equations are clarified.

In this paper, fundamental electric performances such as the input resistance, bandwidth and radiation characteristics are clarified through electromagnetic simulations and experiments. As for a human body tissue, the muscle is selected and a muscle phantom is used for measurements. It is made clear, that the input resistance and the bandwidth are increased by the increase of the human body conductivity, while the antenna gains are decreased.

Index Terms ─ Human body, NMHA, phantom, RF.

I. INTRODUCTION

Recently, radio frequency (RF) sensors inside human bodies have been developed for healthcare applications [1-2]. In implantable RF sensors, small antennas, such as a planar inverted F-antenna and microstrip antenna, were studied [3-4]. In addition, a helical antenna had been used as a very small implantable antenna for a capsule endoscopy system [5-6]. The helical antenna is promising because of its suitable structure for a capsule. However, antenna design method and performances were not made clear. The fundamental design is a self-resonant condition that creates input impedance to pure resistance and achieves higher antenna efficiency. Previously, a structural deterministic equation for a self-resonant condition was developed for ease in practical applications [7]. Researches of NMHA in a human body condition are very limited. Recently, a self-resonant equation in a human body condition was developed [8]. Some studies for input resistance changes and related performance changes were reported [9].

In this paper, fundamental electric performances such as the input resistance, bandwidth and radiation characteristics are clarified through electromagnetic simulations and experiments. In electromagnetic simulations, a commercial simulator FEKO is employed. In calculation, because antenna size is very small such as one tenth of a wavelength and input resistance is less than 0.1 Ω, antenna segment size is optimized to be 1/100 wavelength. The accuracy of simulation results are taken care. As for measurement, a human body phantom is fabricated. The dielectric constants ε_r = 52.7, σ = 0.15 and ε_r = 53.3, σ = 0.89 are achieved. Calculated and measured results of the input impedance, bandwidth and radiation characteristics are compared and good agreements are ensured.

Submitted On: July 17, 2019
Accepted On: December 15, 2019

II. DESIGN EQUATIONS OF NMHA

NMHA have been a well-known antenna. All of its important design equations are nearly clarified in a free space application. However, for use in a human body, equations are still under development. To understand NMHA, present situations are summarized in this chapter. A fundamental performance can be recognized by the equivalent current model shown in Fig. 1 [7].

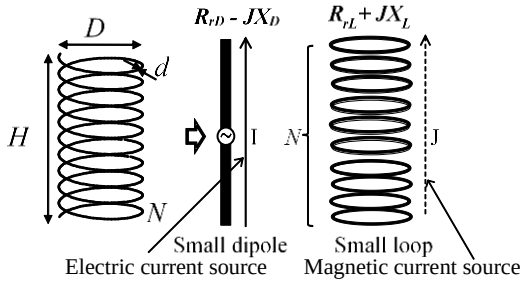

Fig. 1. Equivalent current model of the NMHA.

The coil current is modeled by a straight current and several loop currents. The straight current corresponds to a small dipole with a radiation resistance (R_{rD}) and capacitive reactance (X_D). The loop currents correspond to a small loop with a radiation resistance (R_{rL}) and inductive reactance (X_L). The input impedance is expressed by equation (1):

$$Z_{in} = R_{rD} + R_{rL} + R_l + J(X_L - X_D). \quad (1)$$

Here, R_l expresses the ohmic resistance of the antenna wire. Furthermore, the input resistance (R_{in}) and radiation resistance (R_{rad}) are given as follows:

$$R_{in} = R_{rD} + R_{rL} + R_l, \quad (2)$$

$$R_{rad} = R_{rD} + R_{rL}. \quad (3)$$

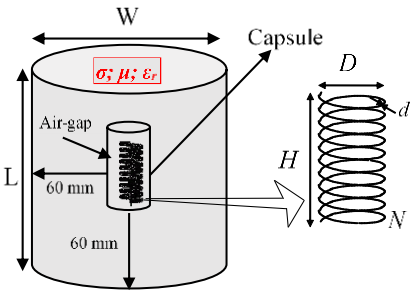

Fig. 2. Simulation model.

The situation of NMHA inside a human body is shown in Fig. 2. NMHA is placed in a capsule and is surrounded by a dielectric material with permittivity and conductivity of ε_r and σ, respectively. The present situations of important equation developments are summarized in Table 1. In a free space condition, all fundamental design equations are clarified. Other electric characteristics relating to impedance matching, stored electromagnetic power, and bandwidth are summarized in paper [10]. In a human body condition, the resistance, reactance, and self-resonant structure are affected by ε_r and σ of the surrounding material. The most important equation for self-resonant structure has already been developed [8], whereas those for resistances are still under development. The equations related to Table 1 are shown in the following.

Table 1: Overview of important design equations

Item		In Free Space	In a Human Body
Resistances	Radiation (R_{rD}; R_{rL}) Ohmic (R_l)	Equations relating to antenna parameters are derived [10]	Equation are under developing
Reactances	Capacitive (X_D) Inductive (X_L)	Equations relating to antenna parameters are derived [7]	Deterministic equation is developed [8]
Self-resonant structure	$X_D = X_L$	Deterministic equation is developed [7]	Deterministic equation is developed [8]

A. In free space

Design equations for R_{rD}, R_{rL} and R_l are expressed as follows:

$$R_{rD} = 20\pi^2 (\frac{H}{\lambda})^2, \quad (4)$$

$$R_{rL} = 320\pi^6 (\frac{D}{2\lambda})^4 N^2, \quad (5)$$

here, λ is the wavelength in free space,

$$R_l = 0.6 \frac{L_t}{d} \sqrt{\frac{120}{\sigma\lambda}}, \quad (6)$$

here, L_t, d and σ are the total length, diameter, and conductivity of antenna wire, respectively.

The capacitive and inductive reactances are expressed as follows [7]:

$$X_D = \frac{279\lambda H_A}{N\pi(0.92H + D)^2}, \quad (7)$$

$$X_L = \frac{600\pi \times 19.7ND^2}{\lambda(9D + 20H)}. \quad (8)$$

The self-resonance is given by $X_D = X_L$ and expressed as follows:

$$\frac{279\frac{H}{\lambda}}{N\pi(0.92\frac{H}{\lambda} + \frac{D}{\lambda})^2} = \frac{600\pi \times 19.7N(\frac{D}{\lambda})^2}{9\frac{D}{\lambda} + 20\frac{H}{\lambda}}. \quad (9)$$

B. In human body

The inductive (X_L) and capacitive (X_D) reactances are expressed as follows [9]:

$$X_L = \omega L_W = \sqrt{\frac{1}{\varepsilon_r}}\frac{600\pi \times 19.7ND^2}{\lambda_g(9D+20H)}, \quad (10)$$

$$X_D = \frac{1}{\omega C} = \sqrt{\varepsilon_r}\frac{125H\lambda_g}{\pi N(1.1H+D)^2}. \quad (11)$$

Here, λ_g is the wavelength in the material and is expressed as follows:

$$\lambda_g = \frac{\lambda_0}{\sqrt{\varepsilon_r \mu_r}}. \quad (12)$$

The self-resonant equation of NMHA is expressed by the equation (13):

$$\sqrt{\frac{1}{\varepsilon_r}}\frac{600\pi \times 19.7N\left(\frac{D}{\lambda_g}\right)^2}{9\frac{D}{\lambda_g}+20\frac{H}{\lambda_g}} = \sqrt{\varepsilon_r}\frac{125\frac{H}{\lambda_g}}{\pi N(1.1\frac{H}{\lambda_g}+\frac{D}{\lambda_g})^2}. \quad (13)$$

III. ELECTROMAGNETIC SIMULATION

A. Simulation model

The simulation model is shown in Fig. 2. NMHA is placed at the center of a dielectric cylinder with radius of 30 mm and height of 60 mm. A very small air gap of 1.0 mm is placed between the antenna and the dielectric material.

B. Simulation parameters

The simulation parameters are summarized in Table 2. The effects of ε_r and σ on the antenna resistances are the main focus. As for a human tissue, a muscle is selected with $\varepsilon_r = 53$, and $\sigma = 0.89$ (S/m) given. To clarify the effect of σ, different values with $\sigma = 0.15$ (S/m) is considered.

Table 2: Simulation parameters

Parameters	Values
Method	FEKO 7.0 (MoM)
Frequency	402 MHz
Wavelength (λ_g)	102.5 (mm)
Dielectric Constant (Muscle)	$\varepsilon_r = 53$, $\mu_r = 1$; $\sigma = 0.15$, 0.89 (S/m); $\rho = 1040$ (kg/m^3)
Segment size of material	$\lambda_g/40$
Number of turns (N)	5; 7; 9
Metallic wire	Copper ($\sigma = 58 * 10^6$ [1/Ωm])
Diameter of Antenna wire (d)	0.5 mm
Segment size of antenna wire	$\lambda_g/100$

For the calculation of the antenna wire and dielectric material, the method of moment (MoM) scheme is used. In order to calculate very small size antenna (between 0.05 λ_g to 0.2 λ_g) and very small input resistances (around 0.1 Ω or less) accurately, segment size of the antenna wire are carefully determined. At the segment size of $\lambda_g/100$, calculated results converged. For a dielectric material, the segment size of $\lambda_g/40$ is selected.

C. Antenna structure

Based on the self-resonant equation of equation (13), the antenna structures are determined. A comparison of the structure obtained from equation (13) and that of simulation results are shown in Fig. 3, where both values conform to each other. The antenna structures are only dependent with ε_r and not with σ. At a given N value, the antenna diameter (D) change is minimal for length (L) changes. This change is similar to that of the compression of a wire spring in which an increase of N, decreases the D. The point A indicate the study antenna structure of D = 8 mm, H = 20 mm, N = 9.

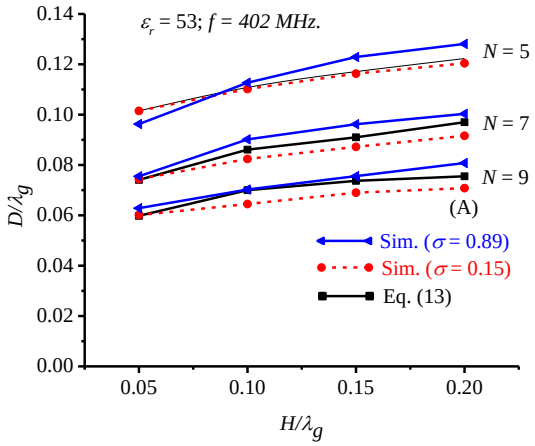

Fig. 3. Comparison of self-resonant structures.

D. Input impedance

The Smith chart display of the input impedance is shown in Fig. 4 and the resistance values are shown in Table 3.

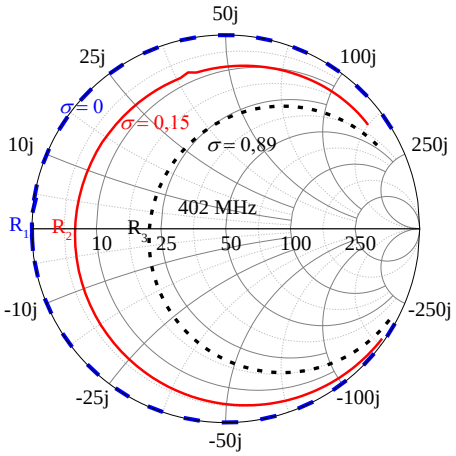

Fig. 4. Antenna input impedance.

Table 3: Antenna resistance value

σ (S/m)	$R_{rD}+R_{rL}$ (Ω)	R_l (Ω)	R_{in} (Ω)
0.00	0.078	0.0357	0.44
0.15	0.078	0.0357	8.58
0.89	0.078	0.0357	22.80

With the increase of σ value, the input resistance is increased. When a low-resistance antenna is placed near a wave absorber, the resistance increases, because the increase of σ corresponds to an increase of wave absorbing ability; there by, a very small resistance at σ = 0 (S/m) is dramatically increased by the increase of σ.

E. Antenna gain

The effects of σ in the radiation characteristics are investigated. The antenna efficiency (η) and antenna gain (G) are shown in Table 4. Here, η is calculated by equation:

$$\eta = \frac{R_{rad}}{R_{in}}, \tag{14}$$

where η is significantly decreased by an-increase in R_{in}, in the case of existence of σ value.

Table 4: Antenna resistance value

σ (S/m)	R_{rad} (Ω)	R_{in} (Ω)	η (%)	η (dB)	G (dBi)
0.00	0.078	0.44	17.93	-7.4	-17.5
0.15	0.078	8.58	0.91	-20.4	-18.7
0.89	0.078	22.80	0.34	-24.7	-24.5

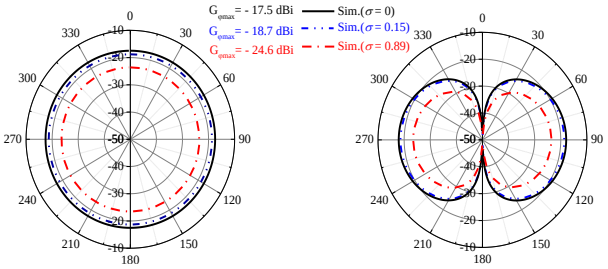

(a) Horizontal plane (b) Vertical plane

Fig. 5. Radiation patterns.

The radiation patterns of the electric field are shown in Fig. 5. In the vertical plane, the radiation pattern forms ***8*** shape. The antenna gain (***G***) is expressed as follows:

$$G = \eta + G_{pat} - L_a \,(\text{dBi}), \tag{15}$$

here, G_{pat} indicates the character ***8*** shape radiation pattern as shown in Fig. 5 (b), G_{pat} becomes 2 dBi. L_a indicates the attenuation of the electromagnetic power through the absorbing material. At σ = 0.15 and σ = 0.89, L_a becomes 1 dB and 3 dB, respectively. So, Antenna gains of 18.7 dBi and 24.5 dBi are considered adequate. In the case of σ = 0, antenna gain is reduced from the η value. In order to investigate this reason, electric field distributions of σ = 0 and σ = 0.15 are obtained as shown in Fig. 6. In the case of σ = 0 shown in Fig. 6 (a), electric field spreads widely out of the antenna. However, the case of σ = 0.15, electric field degradates rapidly out of the antenna. So, reflections caused by the surface impedance mismatch become larger in the case of σ = 0 case. These reflections may become main reason of 10 dB degradation.

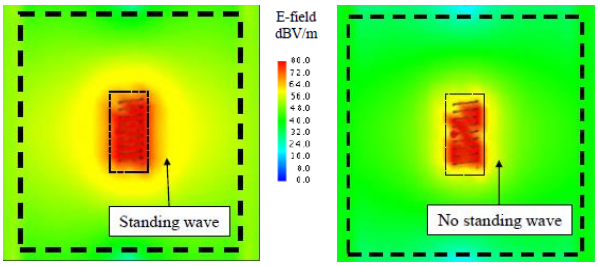

(a) σ = 0 (b) σ = 0.15

Fig. 6. Near field.

IV. EXPERIMENTAL RESULTS

A. Phantom

To measure the antenna electrical characteristics inside a human body, human body phantoms are fabricated, which are composed of chemical powders, such as Agar, Polyethylene, Sodium chloride, Sodium dehydroacetate, monohydrate and Xanthan gum [11-12]. These chemical powders are mixed with distilled water and then heated. To complete a phantom, the heated material is placed in a case. The fabricated phantoms are shown in Fig. 7.

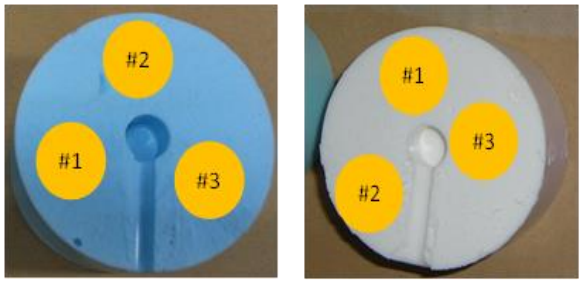

(a) Phan tom 1 (σ = 0.15) (b) Phan tom 2 (σ = 0.89)

Fig. 7. Experiment of phantom.

A round hole and a guide groove are provided for installation of the antenna and feed cable, respectively. Positions #1, #2, and #3 indicate the locations used for the measurement of the dielectric constants, using a dielectric probe kit of Keysight N150/A. With this module, the measured dielectric constant (ε_m) is expressed as a complex value as follows:

$$\varepsilon_m = \varepsilon_r - j\varepsilon_i = \varepsilon_r - j\frac{\sigma}{\omega\varepsilon_0}, \quad (16)$$

here, ε_0 is the permittivity of a vacuum.

Then, σ is obtained by the next expression:

$$\sigma = 2\pi f \varepsilon_i \varepsilon_0. \quad (17)$$

The measured results of ε_r, ε_i, and σ at #1, #2, and #3 locations are summarized in Table 5. In the process of putting the melted phantom in the container, the phantom densitie become different by the cooling speed differences of the phantom parts. To achieve the same value as a muscle (ε_r = 58.8 and σ = 0.84) is rather difficcult. So, the value ε_r = 53.3 and σ = 0.89 is used as a representative of a muscle. For phantom 1, the average values of ε_r and σ are 52.7 and 0.15, respectively. For the phantom 2, the average values of ε_r and σ are 53.3 and 0.89, respectively.

Table 5: Measurement results of phantom

Parameters	Phantom 1			Phantom 2		
	ε_r	ε_i	σ	ε_r	ε_i	σ
#1	54.5	6.8	0.1511	53.0	41.0	0.9111
#2	55.4	7.0	0.1555	52.7	40.8	0.9066
#3	49.0	5.8	0.1288	54.3	39.0	0.8666
Averages	52.7	6.5	0.1450	53.3	40.3	0.8940

B. Input impedance

The measurement set up is shown in Fig. 8. The antenna with a feed cable is set at the center hole and the guide groove as shown in Fig. 8 (a). The antenna size is D = 8 mm, H = 20 mm, N = 9. A plastic insulator is placed between the phantom and antenna with a cable to avoid antenna contact with the phantom.

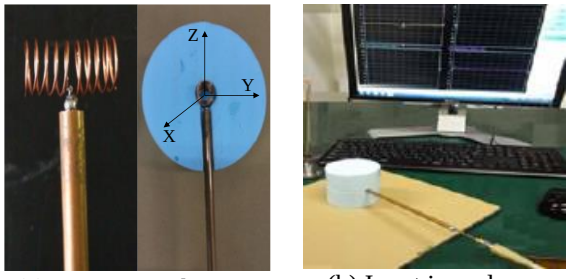

(a) NMHA in phantom (b) Input impedance measurement by VNA

Fig. 8. Experimental of input impedance setup.

For the input impedance measurement shown in Fig. 8 (b), the antenna portion is covered by an upper phantom. The measured input impedances are shown in Fig. 9.

The measured results of σ = 0.15 and σ = 0.89 phantoms conform well to the calculated results. Therefore, the increase of the input resistance using the σ value is ensured in the experiment.

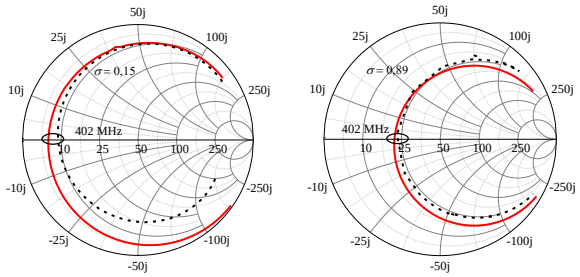

(a) Phantom 1 (σ = 0.15) (b) Phantom 2 (σ = 0.89)

Fig. 9. Input imperdance of NMHA in phantom.

C. Bandwidth

The bandwidth can be expressed by R_{in} as follows. The R_{in} and antenna Q factor are related by equation (18):

$$Q = \frac{X_L}{R_{in}}, \quad (18)$$

here, X_L is the input inductance shown in equation (10) and equation (11).

Then, the bandwidth (BW) at the specified VSWR is expressed by the equation (19):

$$BW = \frac{VSWR - 1}{Q\sqrt{VSWR}}. \quad (19)$$

As a result, BW becomes proportional to R_{in}.

The measured and simulation results of the antenna VSWR characteristics are shown in Fig. 10.

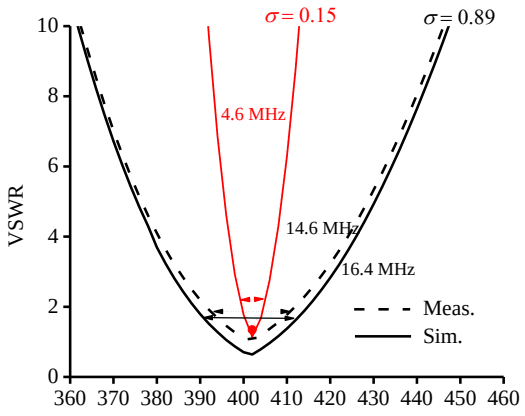

Fig. 10. Comparisons of antenna bandwidth in phantom.

The calculated and measured results at σ = 0.15 and σ = 0.89 conform well to each other. At VSWR = 2, the bandwidth of NMHA in phantom 1 and phantom 2 are 4.6 MHz and 16.4 MHz and correspond to a fractional bandwidth of approximately 1.2% and 4.1%. The bandwidth extensions correspond to the increases of R_{in} in Table 4.

D. Radiation patterns

The set-up of the radiation pattern measurement is shown in Fig. 11. The structure of Fig. 8 (b) that NMHA is covered by a phantom is set on a turntable. The measured antenna is seen in front and the transmission dipole antenna is seen in the opposite side. To measure very small signal level around -20 dBi, the leakage current and reflected wave from the surroundings are carefully reduced. To suppress leakage current on the feeding cable, the cable is covered by a radio wave absorber sheet.

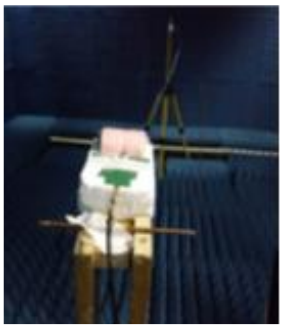

Fig. 11. Experimental of radiation setup.

1). Radiation pattern with phantom 1 (σ = 0.15)

The measured and calculated radiation patterns in the horizontal and vertical planes are shown in Fig. 12 and Fig. 13, respectively. The measured antenna gain is obtained by comparing received levels with the reference half wavelength dipole antenna. Both results agree well at the main polarization and cross polarization.

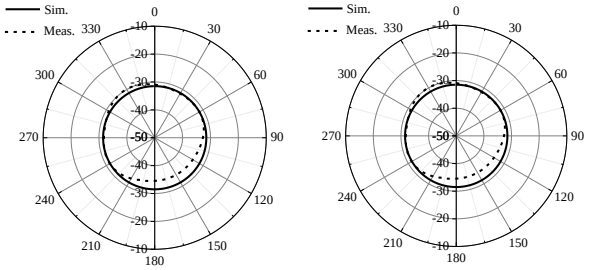

(a) Xross pol. (b) Co-pol.

Fig. 12. Horizontal plane.

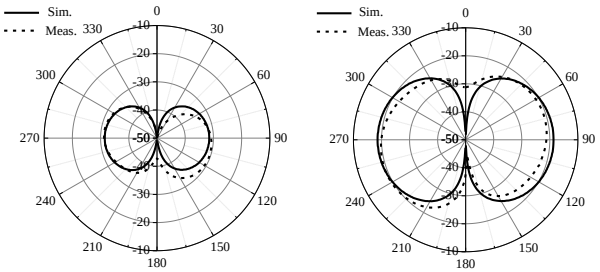

(a) Xross pol. (b) Main pol.

Fig. 13. Vertical plane.

2). Radiation pattern with phantom 2 (σ = 0.89)

The measured and calculated radiation patterns in the horizontal and vertical planes are shown in Fig. 14 and Fig. 15, respectively. Both results agree well at the main polarization and cross polarization.

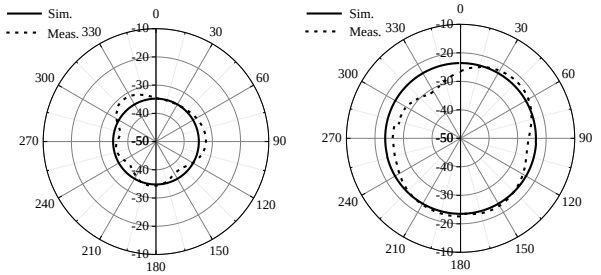

(a) Xross pol. (b) Co-pol.

Fig. 14. Horizontal plane.

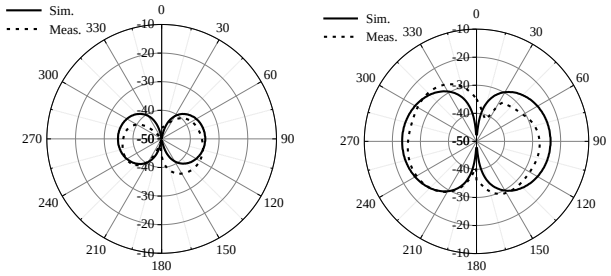

(a) Xross pol. (b) Main pol.

Fig. 15. Vertical plane.

V. CONCLUSIONS

To clarify the electrical characteristics of a normal-mode helical antenna (NMHA) placed in a human body, the change in the input resistance and antenna gain at different conductivity are obtained by simulations and measurements. When the conductivity (σ) is changed: at 0, 0.15, and 0.89 (S/m), the input resistance (R_{in}) become: 0.44, 8.58, and 22.8 (Ω), respectively. With an increase in R_{in}, the antenna efficiency (η) is also changed: -7.4, -20.4, and -24.7 (dBi) for σ = 0, 0.15, and 0.89 (S/m), respectively. The accuracy of the simulated results confirmed through measurement using a human body phantom, and the two results agree well. Thus, a new finding that the input resistance increases as conductivity increases is established.

REFERENCES

[1] ACA, "Planning for medical implant communications systems (MICS) & related devices," Australian Communications Authority, Sydney, NSW, Australia, 2003.

[2] ASGE, "Wireless capsule endoscopy," American Society Gastrointestinal Endoscopy, Downers Grove, IL, USA, 2013.

[3] T. Karacolak, A. Z. Hood, and E. Topsakal,

"Design of a dual-band implantable antenna and development of skin mimicking gels for continuous glucose monitoring," *IEEE Trans. Microw. Theory Techn*., vol. 56, no. 4, pp. 1001-1008, Apr. 2008.

[4] K. Jaehoon and Y. Rahmat-Samii, "Implanted antennas inside a human body: Simulations, designs, and characterizations," *IEEE Trans. Microw. Theory Techn*., vol. 52, no. 8, pp. 1934-943, Aug. 2004.

[5] J. Faerber, et al., "In vivo characterization of a wireless telemetry module for a capsule endoscopy system utilizing a conformal antenna," *IEEE Trans. Biomed. Circuits Syst.*, vol. 12, no. 1, pp. 95-105, Feb. 2018.

[6] C. Liu, Y. X. Guo, and S. Xiao, "Circularly polarized helical antenna for ISM-band ingestible capsule endoscope systems," *IEEE Trans. Antennas Propag*., vol. 62, no. 12, pp. 6027-6039, Dec. 2014.

[7] N. Q. Dinh, N. Michishita, Y. Yamada, and K. Nakatani, "Deterministic equation for self-resonant structures of very small normal-mode helical antennas," *IEICE Trans. Commun*., vol. E94-B, no. 5, pp. 1276-1279, May 2011. Online ISSN: 1745-1345, Print ISSN: 0916-8516.

[8] N. T. Tuan, Y. Yamada, N. Q. Dinh, R. H. M. Baharin, K. B. Kamardin, D. T. Dung, and N. Michishita, "Deterministic equation of self resonant structures for normal-mode helical antennas implanted in a human body," *IEEE Antennas and Wireless Propagation Letters*, vol. 17, no. 8, pp. 1377-1381, Aug. 2018. Print ISSN: 1536-1225, Online ISSN: 1548-5757, DOI: 10.1109/LAWP.2018.2846600.

[9] N. T. Tuan, M. B. R. Hanan, Y. Yamada, D. T. Dung, N. Q. Dinh, and N. Michishita, "Radiation characteristics of small nomal-mode helical antenna for internal human body sensing," *IIEEJ-International Workshop on Image Electronics and Visual Computing*, General session 5A-3, Danang, Vietnam, Mar. 2017.

[10] D. T. Dung, N. Q. Dinh, D. Q. Trinh, and Y. Yamada, "Investigating equations used to design very small normal-mode helical antenna in free space," *International Journal of Antennas and Propagation*, vol. 2018, Article ID 7967468, 7 pages, DOI: 10.1155/2018/7967468.

[11] C. Gabriel, "Compilation of the dielectric properties of body tissues at RF and microwave frequencies," Technical Report AL/OE-TR-1996-0037, Brooks Air Force.

[12] T. Takimoto and T. Onishi, "Characteristics of biological tissues equivalent phantoms applied to UWB communications," *IEICE Trans*., pp. 1674-1681, 2005.

N. Q. Dinh is currently an Associate Professor at Faculty of Radio-Electronics Engineering, Le Quy Don Technical University Vietnam. He received the B.E, M.E. and D.E. degrees in Department of Electrical & Electronic Engineering, National Defense Academy, Yokosuka, Japan, in 2006, 2008, and 2011, respectively. Since 2011, he has been a Research Associate at the Faculty of Radio-Electronics Engineering, Le Quy Don Technical University, Hanoi, Vietnam. His research interests include very small antennas, array antennas, UWB antennas, and MIMO antennas, BTS antennas. He is a member of the Institute of Electronics, Information and Communication Engineers (IEICE), Japan. He was the recipient of the Young Scientist Award of the IEICE Antennas and Propagation Society Japan Chapter, Japan (2011).

D. T. Dung received the B.E degree in Electronic Engineering from Le Quy Don Technical University, Hanoi, Viet Nam in 2006, and M.E in Telecommunications Engineering from Posts and Telecommunications Institute of Technology, Hochiminh, Viet Nam in 2011. He is currently working for Telecommunication University, Khanhhoa, Vietnam. His research interest include antenna for medical application, very small antennas.

Y. Yamada received the B.E. and M.E. degrees on Electronics from Nagoya Institute of Technology, Nagoya, Japan in 1971 and 1973, respectively. And he received the D.E. degree on Electrical Engineering from Tokyo Institute of Technology, Tokyo, Japan in 1989. In 1973, he joined the Electrical Communication Laboratories of Nippon Telegraph and Telephone Corporation (NTT). Till 1984, he was engaged in research and development of reflector antennas for terrestrial and satellite communications. From 1985, he engaged in R&D of base station antennas for mobile radio systems. In 1993, he moved to NTT Mobile Communications Network Inc. (NTT DoCoMo). In 1995, he was temporarily transferred to YRP Mobile Telecommunications Key Technology Research Laboratories Co., Ltd. At the same time, he was a Guest Professor of the cooperative research center of Niigata University, and a Lecturer of Science University of Tokyo, both from 1996 to 1997. In 1998, he changed his occupation to a Professor of National Defense Academy, Kanagawa, Japan. In 2014,

he had started working as a Professor at Malaysia-Japan International Institute of Technology, Universiti Teknologi Malaysia, Kuala Lumpur, Malaysia. Now, he is interested in very small antennas, array antennas, aperture antennas and electromagnetic simulation of radar cross section. He received the best paper award and the best tutorial paper award from IEICE in 2013 and 2014, respectively. He is a Fellow member of the IEICE and a member of JSST of Japan. He is also a senior member of IEEE AP society and a member of the ACES.

N. Michishita received the B.E., M.E., and D.E. in Electrical and Computer Engineering from Yokohama National University in 1999, 2001, and 2004, respectively. He joined the Department of Electrical and Electronic Engineering, National Defense Academy, as a Research Associate in 2004, and currently holds the title of Associate Professor. He was a Visiting Scholar at the University of California, Los Angeles, from 2006 to 2007. He received the Young Engineer Award from the IEEE AP-S Japan Chapter and IEICE in 2004 and 2005, respectively. His current research interests include metamaterial antennas and electromagnetic analysis. He is a member of the IEEE.